The layered compound CaClFeP is an Arsenic-free high T_c iron-pnictide

Xun-Wang Yan[1,2] and Zhong-Yi Lu[2*]
[1] *Institute of Theoretical Physics, Chinese Academy of Sciences, Beijing 100190, China and*
[2] *Department of Physics, Renmin University of China, Beijing 100872, China*
(Dated: October 5, 2010)

We first analyze why the iron pnictides with high T_c superconductivity so far are As-based, by the Hund's rule correlation picture, then examine the P-based and Sb-based cases, respectively. Consequently, we propose that CaClFeP with ZrCuSiAs-type structure is an As-free high T_c iron-pnictide. The subsequent density functional theory calculations show that the ground state of CaClFeP is of a collinearly antiferromagnetic order on Fe moments with structural distortion, resulting from the interplay between the strong nearest and next-nearest neighbor antiferromagnetic superexchange interactions bridged by P atoms, similar as the As-based pnictides. The other P-based pnictides are either nonmagnetic or magnetic but with weak exchange interactions. The Sb-based pnictides unlikely show high T_c superconductivity because of the existence of robust ferromagnetic order.

PACS numbers: 74.70.Xa, 74.20.Pq, 74.20.Mn

The discovery of high transition temperature T_c superconductivity in LaOFeAs by partial substitution of O with F atoms [1] stimulates the intense studies on the iron pnictides. Upon doping or high pressure, there are three types of iron pnictides reported to show superconductivity, i.e. 1111-type ReOFeAs (Re = rare earth) [1] or BaFFeAs and SrFFeAs [2], 122-type AFe$_2$As$_2$ (A=Ba, Sr, or Ca) [3], and 111-type BFeAs (B = alkali metal) [4]. All these pnictides share the same structural feature that there exist the robust tetrahedral layers where the Fe atoms are tetragonally coordinated by the As atoms and the superconduction pairing may happen.

To our knowledge, all the iron pnictides showing high T_c superconductivity so far are As-based. Here the high T_c means close to or above the theoretical maximum value of 40K predicted from BCS theory[5] so that the corresponding superconductors are considered unconventional. Up to now, the highest T_c reported in As-free pnictides is 17K shown in $(Fe_2P_2)(Sr_4Sc_2O_6)$ [6]. Is it possible to find a P- or Sb-based pnictide without As to show high T_c superconductivity? Physically to answer this question essentially depends upon how we understand the mechanism underlying the high T_c superconductivity in the pnictides. Likewise, solving this question will greatly help us to understand the underlying mechanism. Moreover, setting of this issue is very meaningful and important in practice because Arsenic strong toxicity sets the strict safety conditions to synthesize As-based pnictide samples, which confine the samples making in a few research groups worldwide. In this Letter, we show that CaClFeP with the ZrCuSiAs-type structure is an As-free high T_c pnictide with the similar electronic structure and magnetic property as the As-based pnictides.

It was universally found that all the As-based pnictides are in a collinear antiferromagnetic (AFM) order below a tetragonal-orthorhombic structural transition temperature [7, 8]. Accordingly, the superconducting pairing in the As-based pnictides is now considered as being mediated by the spin fluctuations. Regarding the mechanism behind the structural and AFM transitions and their underlying relationship, there are basically two contradictive views, based on the itinerant electron picture [9] and the local moment picture [10–12] respectively. From the very beginning, we proposed [12] the fluctuating Fe local moments with the As-bridged AFM superexchange interactions as the driving force upon the two transitions, effectively described by the J_1-J_2 Heisenberg model. Here we would like to emphasize the twofold meanings in our proposal [12]: (1) there are localized magnetic moments around Fe ions and embedded in itinerant electrons in real space; (2) it is those bands far from rather than nearby the Fermi energy that determine the magnetic behavior of the As-based pnictides, namely the hybridization of Fe with the neighbor As atoms plays a substantial role. Here the formation of a local moment on Fe ion is mainly due to the strong Hund's rule coupling on the Fe 3d-orbitals, which is about 0.6-0.8 eV/Fe[12]. In this sense, our proposal can be referred to as the Hund's rule correlation picture. We emphasize again that the Arsenic atoms play a substantial role in our physical picture. Based on this Hund's rule correlation picture, we had successfully predicted [13] that the ground state of α-FeTe is in a bi-collinear AFM order, which was confirmed by the later neutron scattering experiment [14].

The main factor competing with the Hund's rule coupling is the chemical bonding between the Fe 3d orbitals and As 4p orbitals. Meanwhile the hybridization between the Fe 3d orbitals and As 4p orbitals will bridge the superexchange interactions between the Fe magnetic moments induced by the Hund's rule coupling. It is thus a dilemma to require strong superexchange interactions with robust Fe magnetic moments. Chemically, the spin-degenerated Fe 3d orbitals form stronger bonds with the As 4p orbitals than the spin-polarized Fe 3d orbitals do. For the As-based pnictides, inspection of the calculations [12] shows that the spin degeneration pushes down the en-

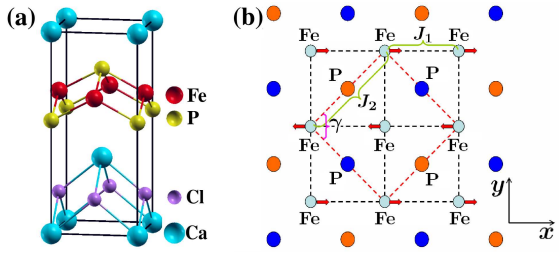

FIG. 1: (Color online) CaClFeP with the ZrCuSiAs-type structure: (a) a tetragonal unit cell containing two formula units; (b) schematic top view of the FeP layer. The small red dashed square is an $a \times a$ unit cell, while the large black dashed square is a $\sqrt{2}a \times \sqrt{2}a$ unit cell. The Fe spins in the collinear antiferromagnetic order are shown by the red arrows.

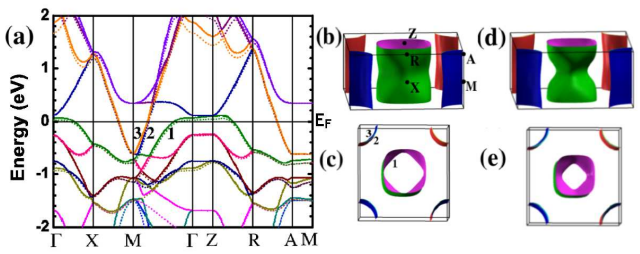

FIG. 2: (Color online) CaClFeP in the nonmagnetic state: (a) energy band structure, in which solid lines for the undoping while dotted lines for the 10%-replacement of Ca by La; (b) the Fermi surface; (c) top view on the Fermi surface. (d) and (e) correspond to the case of 10%-replacement of Ca by La.

ergy levels raised by the Hund's rule coupling, and then strengthens the bonding between the Fe $3d$ orbitals and As $4p$ orbitals, which makes substantial energy gain to the nonmagnetic state. However, this is still not enough to completely overcome the Hund's rule coupling, in need of an additional energy gain of ∼0.2 eV/Fe, as suggested by calculated total energy difference between the nonmagnetic state and collinear AFM state [12]. Consequently, there are magnetic moments induced around Fe atoms with the AFM superexchange interactions bridged by the As atoms.

In line of pnicogen atoms of P, As, and Sb, P has a much smaller atomic radius with a larger electronegativity than As while Sb has a much larger atomic radius with a smaller electronegativity than As. Hence, it is very likely that in the most P-based pnictides there will form a very strong bonding between P and Fe so that the Hund's rule coupling is quenched. This is verified by the calculations reported below that the most P-based pnictides are nonmagnetic. On the other hand, in the most Sb-based pnictides there will form a relatively weak bonding between Sb and Fe so that large moments are induced around Fe atoms with robust ferromagnetic spin fluctuations, which is also verified by the calculations reported below. In contrast, Arsenic is in a proper balance to the dilemma. This explains why the iron pnictides with high T_c superconductivity, discovered so far, are As-based rather than P-based or Sb-based. Now we deduce that if the in-plane lattice parameters a and b of a P-based (Sb-based) pnictide are more large (small), its electronic structure and magnetic property are more similar to the ones of the As-based pnictides since the P-Fe (Sb-Fe) bonding is more weakened (strengthened). Referring to the As-based pnictides, we further deduce that CaClFeP has the magnetic structure and property similar to the ones of the As-based pnictides, in great possibility to realize the high T_c superconductivity.

To verify the deduction, we carried out the density functional theory (DFT) electronic structure calculations. In the calculations the plane wave basis method was used [15]. We adopted the generalized gradient approximation (GGA) of Perdew-Burke-Ernzerhof [16] for the exchange-correlation potentials. The ultrasoft pseudopotentials [17] were used to model the electron-ion interactions. After the full convergence test, the kinetic energy cut-off and the charge density cut-off of the plane wave basis were chosen to be 600eV and 4800eV, respectively. The Gaussian broadening technique was used and a k-mesh of $16 \times 16 \times 8$ or $12 \times 12 \times 8$ was adopted to sample the Brillouin zone of $a \times a \times c$ or $\sqrt{2}a \times \sqrt{2}a \times c$ supercell, respectively. In the calculations, the lattice parameters with the internal atomic coordinates were all determined by the energy minimization. CaClFeP is in a tetragonal layered structure with $P4/nmm$ symmetry. A crystal unit cell consists of eight atoms with alternating FeP and CaCl layers along the c axis (Fig. 1(a)).

As analyzed above, our calculations show that 111-type BFeP (B = Li or Na) and 122-type AFe$_2$P$_2$ (A=Ba, Sr, or Ca) are all nonmagnetic semimetals since the strong Fe-P bonding quenches the Fe magnetic moments. Actually, the lattice parameters a and b of these compounds are mainly determined by FeP layers, around 3.8 Å. The large parameters a and b go to the 1111-type, in which the other layers strongly affect the lattice parameters. Indeed, we find the large lattice parameters (a=b=4.14 Å, c=8.70 Å) for CaClFeP in magnetic phases.

In Fig. 2 we plot the electronic band structure and Fermi surface of CaClFeP in the nonmagnetic state. There are three cylinder-like Fermi surface sheets, among which the two are of electron-type around M-A and the other one is of hole-type around Γ-Z. The volumes enclosed by these Fermi sheets give 0.19 electrons/cell and equally 0.19 holes/cell, i.e. $1.31 \times 10^{21}/\mathrm{cm}^3$. The compound CaClFeP is thus a semimetal with a low carrier density, between normal metals and semiconductors. The density of states (DOS) at the Fermi energy is 3.65 states/(eV× unit cell). The corresponding electronic specific heat coefficient $\gamma = 8.60\ mJ/(K^2 * mol)$ and the Pauli paramagnetic susceptibility $\chi_p = 1.49 \times 10^{-9}\ m^3/mol$. The 10%-replacement of Ca by

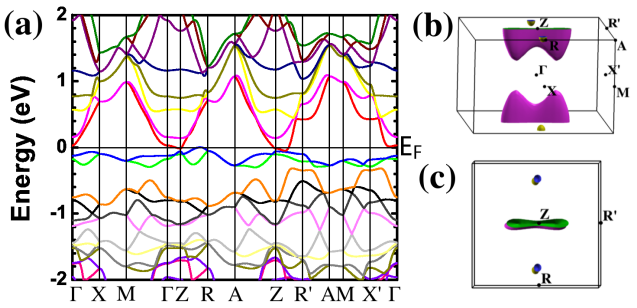

FIG. 3: (Color online) CaClFeP in the collinear-ordered antiferromagnetic state with the in-plane angle $\gamma = 90.4^\circ$ (see Fig. 1(a)): (a) energy band structure; (b) the Fermi surface; (c) top view on the Fermi surface. Notice that ΓX corresponds to the parallel-aligned moment line while $\Gamma X'$ corresponds to the antiparallel-aligned moment line.

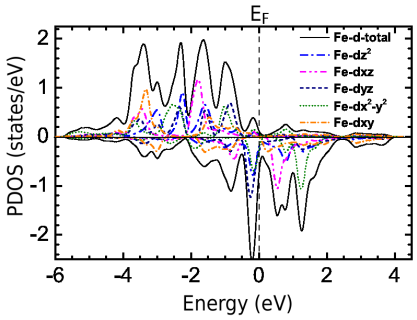

FIG. 4: (Color online) Calculated total and projected density of states at the five Fe-3d orbitals around one of the four Fe atoms in the collinear antiferromagnetic state unit cell.

La makes the electron-type and hole-type Fermi sheets more matched in shape, as shown in Fig. 2 (d) and (e).

In order to explore the magnetic structures and clarify the exchange interactions between the Fe-Fe moments, we calculated three different magnetic states, the ferromagnetic, checkerboard (Neel) AFM, and collinear AFM states, which respective energies are calculated to be (0.040, -0.044, -0.132) eV/Fe if the energy of the nonmagnetic state is set to zero. The magnetic moment around each Fe atom is found about $2.0\mu_B$. All these magnetic states can be self-consistently described by the following frustrated Heisenberg model with the nearest and next-nearest neighbor couplings J_1 and J_2,

$$H = J_1 \sum_{\langle ij \rangle} \vec{S}_i \cdot \vec{S}_j + J_2 \sum_{\ll ij \gg} \vec{S}_i \cdot \vec{S}_j, \qquad (1)$$

whereas $\langle ij \rangle$ and $\ll ij \gg$ denote the summation over the nearest and next-nearest neighbors, respectively. From the calculated energy data, we find that $J_1 \sim 20.96\ meV/S^2$ and $J_2 \sim 32.58\ meV/S^2$ (the detailed calculation is referred to Appendix of Ref. 12). The ground state of CaClFeP is thus in a collinear AFM order.

In the collinear AFM phase, a small structural distortion is found to further make energy gain by 1.2 meV/Fe, which changes the angle between two principal axes in ab-plane γ from 90° to 90.4° (see Fig. 1(b)), equivalently, the lattice unit cell slightly expands along the spin-antiparallel direction and slightly shrinks along the spin-parallel direction. Here we emphasize that our calculations show that the driving force upon this tetragonal-orthorhombic structural distortion is nothing but the magnetic interaction. More specifically it is the superexchange interaction J_2 that induces the Fe-spin collinear AFM order and drives the structural distortion to break the rotational symmetry, as found in LaOFeAs [12]. Moreover, the anti-parallel alignment for the Fe moments between the neighboring FeP-layers was found almost degenerate with the parallel alignment.

TABLE I: Calculated exchange couplings J_1-J_2 (Fig. 1(b)) with measured superconductivity transition temperature T_c.

	J_1 (meV/Fe)	J_2 (meV/Fe)	T_c (K)
LaOFeP	0.52	7.83	7[6]
$(Fe_2P_2)(Sr_4Sc_2O_6)$	3.74	12.24	17[21]
BaFFeP	0.62	11.20	?
CaClFeP	20.96	32.58	?

From Fig. 3, we notice that the Fermi surface is more distributed along ZR' or $\Gamma X'$ than along ZR or ΓX direction in Brillouin zone for CaClFeP in the collinear AFM state, similar as in LaOFeAs and $BaFe_2As_2$[12, 18]. This suggests that the spin-antiparallel direction is more conductive than the spin-parallel direction in real space. This anti-intuitive finding was confirmed by the recent experiment on the detwinned $BaFe_2As_2$ [19].

Fig. 4 projects the density of states onto the five 3d orbitals of Fe in the collinear AFM of CaClFeP. We see that the five up-spin orbitals are almost filled while the five down-spin orbitals are nearly uniformly partially filled. This shows that the P atom-imposed crystal field splitting is small. The formation of Fe magnetic moments is thus due to the Hund's rule coupling, which is a universal feature found in all the As-based pnictides [12, 18].

Other 1111-type P-based pnictides were also calculated. They all show the similar electronic structures and magnetic properties but with much smaller exchange couplings, as reported in Table I. These compounds have smaller lattice parameters (about 4 Å) than CaClFeP.

We have known that all the As-based pnictides have the similar electronic structures and magnetic properties. Upon doping or high pressure, the AFM long-range order is suppressed. The remanent AFM fluctuations are now considered to be responsible for the superconducting pairing in pnictides [12], similar as in cuprate superconductors. We had systematically calculated the exchange couplings J_1 and J_2 for the different As-based pnictides. And we found that phenomenologically the superconduc-

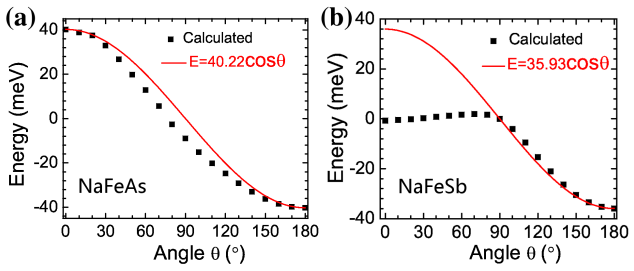

FIG. 5: (Color online) Calculated magnetic energy versus the angle θ between the two sublattice spin orientations, from the ferromagnetic order ($\theta = 0°$) to the Neel AFM order ($\theta = 180°$). (a) NaFeAs and (b) NaFeSb.

tivity transition temperature T_c is proportional to J_2[18]. Theoretically, the two-band t-J_1-J_2 model also indicates that the T_c in pnictides is proportional to the J_2[20].

As we have just shown, CaClFeP takes the similar electronic structure and magnetic property as the As-based pnictides and the exchange couplings J_1 and J_2 of it are as large as the ones of $BaFe_2As_2$ [18]. We thus predict that the high T_c (likely over 40K) superconductivity can be realized in CaClFeP. Meanwhile, for LaOFeP and $(Fe_2P_2)(Sr_4Sc_2O_6)$ the smallness of calculated J_1 and J_2 is consistent with the observed low T_c (Table I).

We have performed the DFT calculations on Sb-based pnictides, including 111-type, 122-type, and 1111-type compounds. We find that all these Sb-based pnictides are similar with each other in electronic structures and magnetic properties. In magnetic states, they show rich magnetic orders like the checkerboard AFM, bi-collinear AFM, and collinear AFM orders, however, there are much larger moments formed at Fe atoms ($\sim 3\mu_B$/Fe) in the Sb-based pnictides than in the As-based pnictides because of the strong Hund's rule effect and the weak Fe-Sb bonding, as analyzed above. Besides, even though the collinear AFM order is the most stable energetically, there exists a stable ferromagnetic order in the Sb-based pnictides, independent of the AFM fluctuations. This is essentially different from the As-based pnictides, in which a ferromagnetic order is never stable.

Fig. 5(a) shows that for NaFeAs the ferromagnetic order is a maximum energetically, and the magnetic energy versus the angle θ between the two sublattice spin orientations is well described by the nearest neighbor exchange Heisenberg model. The calculations also show that CaClFeP behaves likewise. In contrast, for NaFeSb the ferromagnetic state is a local minimum in the energy landscape, lower than the nonmagnetic state (Fig. 5(b)). And the variation of the magnetic energy with the angle θ severely deviates from the exchange Heisenberg model. This shows that the ferromagnetic state has a different exchange interaction origin than the AFM states, which is likely related to the possible orbital ordering. This ferromagnetic state can be stable until applying a high pressure of 25 GPa. Since such ferromagnetic correlations are against the superconducting pairing induced by the AFM fluctuations, we don't think there is the high T_c superconductivity realized in Sb-based pnictides. To our knowledge, no Sb-based pnictides are reported to show high T_c superconductivity in experiment.

In summary, by the Hund's rule correlation picture we may well understand the iron pnictides, in which the different magnetic structures and properties result mainly from the competition between the Hund's rule effect on Fe 3d-orbitals and the Fe-P, Fe-As, or Fe-Sb bonding. In search for an As-free high T_c pnictide, we show that CaClFeP is an AFM semimetal with the strong P-bridged nearest and next-nearest neighbor AFM superexchange interactions, which give rise to the collinear AFM order on Fe moments in the ground state, similar as LaOFeAs and $BaFe_2As_2$. Upon doping or high pressure, CaClFeP is predicted to show high T_c superconductivity. The other 1111-type P-based iron-pnictides are also AFM semimetals but with weak exchange interactions, while both 111-type and 122-type P-based iron-pnicitdes are nonmagnetic semimetals. We also show that the Sb-based pnictides unlikely show high T_c superconductivity.

This work is supported by National Natural Science Foundation of China and by National Program for Basic Research of MOST, China.

* Electronic address: zlu@ruc.edu.cn

[1] Y. Kamihara, *et al.*, J. Am. Chem. Soc. **130**, 3296 (2008).
[2] M. Tegel, *et al.*, Europhys. Lett. **84**, 67007 (2008); X. Zhu, *et al.*, Europhys. Lett. **85**, 17011 (2009).
[3] M. Rotter *et al.*, Phys. Rev. Lett. **101**, 107006 (2008).
[4] X. C. Wang *et al.*, Solid State Commun. **148**, 538 (2008).
[5] W.L. McMillan, Phys. Rev. **167**, 331 (1968).
[6] Y. Kamihara, *et al.*, J. Am. Chem. Soc. **128**, 10012 (2006).
[7] C. de la Cruz *et al.*, Nature (London) **453**, 899 (2008).
[8] J. Dong *et al.*, Europhys. Lett. **83**, 27006 (2008).
[9] I.I. Mazin, *et al.*, Phys. Rev. Lett. **101**, 057003 (2008).
[10] T. Yildirim, Phys. Rev. Lett. **101**, 057010 (2008).
[11] Q. Si and E. Abrahams, Phys. Rev. Lett. **101**, 076401 (2008).
[12] F. Ma, Z.Y. Lu, and T. Xiang, Phys. Rev. B **78**, 224517 (2008).
[13] F. Ma *et al.*, Phys. Rev. Lett. **102**, 177003 (2009).
[14] S.L. Li, *et al.*, Phys. Rev. B **79**, 054503 (2009).
[15] P. Giannozzi *et al.*, http://www.quantum-espresso.org.
[16] J.P. Perdew, K. Burke and M. Ernzerhof, Phys. Rev. Lett. **77** 3865 (1996).
[17] D. Vanderbilt, Phys. Rev. B **41**, 7892 (1990).
[18] F. Ma, Z.Y. Lu, and T. Xiang, Front. Phys. China, **5(2)**, 150 (2010).
[19] M.A. Tanatar, *et al.*, Phys. Rev. B **81**, 184508 (2010).
[20] K. Seo, A. B. Bernevig, J. Hu, Phys. Rev. Lett. **101**, 206404 (2008).
[21] H. Ogino, *et al.*, Supercond. Sci. Technol. **22**, 075008 (2009).